



HAL
open science

Rotational excitation of CO₂ induced by He: New potential energy surface and scattering calculations

A Godard Palluet, Franck Thibault, François Lique

► To cite this version:

A Godard Palluet, Franck Thibault, François Lique. Rotational excitation of CO₂ induced by He: New potential energy surface and scattering calculations. *Journal of Chemical Physics*, 2022, 156 (10), pp.104303. 10.1063/5.0085094 . hal-03632769

HAL Id: hal-03632769

<https://hal.science/hal-03632769>

Submitted on 12 Apr 2022

HAL is a multi-disciplinary open access archive for the deposit and dissemination of scientific research documents, whether they are published or not. The documents may come from teaching and research institutions in France or abroad, or from public or private research centers.

L'archive ouverte pluridisciplinaire **HAL**, est destinée au dépôt et à la diffusion de documents scientifiques de niveau recherche, publiés ou non, émanant des établissements d'enseignement et de recherche français ou étrangers, des laboratoires publics ou privés.

Sample title

Rotational excitation of CO₂ induced by He: New potential energy surface and scattering calculations

A. Godard,^{1, a)} F. Thibault,¹ and F. Lique^{1, a)}*Université de Rennes 1, CNRS, IPR (Institut de Physique de Rennes) - UMR 6251, F-35000 Rennes, France*

(*Electronic mail: amelie.godard@univ-rennes1.fr)

(*Electronic mail: franck.thibault@univ-rennes1.fr)

(*Electronic mail: francois.lique@univ-rennes1.fr)

(Dated: 8 February 2022)

The CO₂ molecule is of great interest for astrophysical studies since it can be found in a large variety of astrophysical media where it interacts with the dominant neutral species such as He, H₂ or H₂O. The CO₂-He collisional system was intensively studied over the last two decades. However, collisional data appear to be very sensitive to the potential energy surface (PES) quality. Thus, we provide in this study a new PES of the CO₂-He van der Waals (vdW) complex calculated with the coupled cluster method and a complete basis set extrapolation in order to provide rotational rate coefficients as accurate as possible. The PES accuracy was tested through the calculations of bound state transition frequencies and pressure broadening coefficients that were compared to experimental data. An excellent agreement was globally found. Then, revised collisional data were provided for the 10 - 300 K temperature range. Rate coefficients were compared to previously computed ones and are found to be up to 50% greater than previously provided ones. These differences can induced non-negligible consequences for the modeling of CO₂ abundance in astrophysical media.

I. INTRODUCTION

Interacting systems implying the CO₂ molecule are of great interest for astrophysical studies. Indeed, CO₂ can be found in various astrophysical media, such as the interstellar medium,¹ protoplanetary disks,² and in planetary and cometary atmospheres.³ It is also a major components of interstellar and cometary ice mantles.⁴

In these media, *in situ* measurements are very complicated if not impossible. Therefore, the analysis of their chemical compositions and physical conditions is made through the interpretation of spectra captured by telescopes.

The spectral analysis requires to know the population of the molecular energy levels.⁵ Most of the astrophysical media are not at the local thermodynamic equilibrium (LTE), so that the population of molecular energy levels is no longer following a Maxwell-Boltzmann distribution. It is then evaluated by a radiative transfer model analysis, taking into account both radiative and collisional (de)excitations. Radiative processes are characterized by Einstein coefficients, for which analytical formula exists, and collisional processes are characterized by the so-called rate coefficients, which are collisional-system-specific.⁵ Such rate coefficients are obtained from scattering calculations based on a potential energy surface (PES) describing the interactions between the two colliders.

The CO₂ molecule is detected through ro-vibrational transitions due to its lack of dipole moment.⁴ Since a non-LTE distribution of the rovibrational energy levels is expected to occur in cold astrophysical media, collisional data for both rotational and ro-vibrational transitions are needed. Note that,

despite the absence of electric dipole moment, non-LTE effects are still predicted to occur at low density ($n < 10^4 \text{ cm}^{-3}$) for the lowest rotational states in the fundamental vibrational level.² As a first estimate, ro-vibrational data can be estimated from pure rotational ones⁶. It is then crucial to provide accurate collisional data for the CO₂ molecule.

Helium is an important collider in astrophysical media and rate coefficients involving helium can be used to infer those for para-H₂($j = 0$) through an adequate scaling factor involving the reduced mass.⁵

CO₂-He rate coefficients were provided for only 5 rotational levels (up to $j = 8$) by Yang & Stancil⁷ based on Ran & Xie⁸ PES. The latter computed their PES with the coupled cluster single double and perturbative triple excitations method (hereafter CCSD(T)) and the augmented correlation-consistent quadruple-zeta (hereafter aVQZ) basis set with additional mid-bond functions. Despite an already accurate PES, larger basis set are now reachable in terms of computational times. Moreover, mid-bond functions as used for the computation of Ran & Xie PES can introduce an overestimation of the potential energy and an inhomogeneous accuracy.⁹ As collisional data are very sensitive to the PES, especially at low energy,^{7,10,11} it is of the utmost importance to provide a PES as accurate as possible. Therefore, we decided to compute a new one with the gold standard CCSD(T) method and an extrapolation to the complete basis set.¹²

This new PES was then used to run scattering calculations using a full close-coupling (CC) approach in order to provide new highly accurate rotational state-to-state rate coefficients involving 21 rotational levels (up to $j = 40$) for the 10 - 300 K range of temperature of great interest for astrophysical modeling of the CO₂ molecule.

The presentation of our work starts in Section II by a summary of the previous studies on the CO₂-He collisional

^{a)} Also at LOMC (Laboratoire des ondes et milieux complexes), Université du Havre & CNRS, Normandie Université, F-76063 Le Havre, France

system from a theoretical and experimental point of view. Section III presents the computational methods used to obtain the PES (Section III A), bound states (Section III B) and scattering data (Section III C).

In Section IV, a description of the PES is included and its comparison with previously computed PESs will be discussed. The accuracy of the surface is then validated in Section V through comparison between computed and experimental bound state transition frequencies and pressure broadening coefficients in Section V.A and V.B, respectively. New collisional data such as inelastic cross sections and rate coefficients are presented in Section VI.A. In addition, the sensitivity of collisional data with respect to the PES will be discussed through the comparison of rate coefficients previously published by Yang & Stancil⁷ based on Ran & Xie PES.⁸ Furthermore, our cross sections will be compared in Section VI.B to the ones of al-Qady *et al.*,¹³ provided in their study on cold collisions between helium and highly rotationally excited CO₂. Finally, conclusions are drawn.

II. PREVIOUS WORK ON CO₂-HE INTERACTING SYSTEM

During the 70s, the success of the simple electron gas model¹⁴⁻¹⁶ renewed the interest into interaction energies calculations in vdW complexes. In order to investigate the angular dependence on such energies in these systems, Parker *et al.*¹⁷ used this method to obtain the earliest realistic 2D-PES of the CO₂-He collisional system, where vibrational motions were ignored.

Based on this surface, Parker *et al.*¹⁸ performed vibrational close-coupling rotational infinite order sudden (VCC-IOS) scattering calculations. They obtained rate coefficients which they assumed to be accurate for temperatures above 300 K.

An empirical CO₂-He PES was then established by Keil *et al.*¹⁹ It was obtained through central field and anisotropic parametrizations based on deconvolution of molecular-beam total differential cross sections.

Few years after, Stroud & Raff²⁰ provided a full *ab initio* PES computed with the self-consistent field (SCF) method. The CO₂ molecule was considered as a rigid-rotor with a C—O bond taken to 2.1942 a_0 . This PES was in reasonable agreement with the two former ones. In order to study its accuracy, Stroud & Raff²⁰ computed rate coefficients, state-to-state cross sections, and differential cross sections with about 28 500 quasiclassical trajectories on their *ab initio* PES, and the ones of Parker *et al.*¹⁷ and Keil *et al.*¹⁹ It was then highlighted that long-range attractive forces are of crucial importance on scattering processes at low collisional energy. However, at high energy the potential well is no longer an important topological feature, unlike the curvature and slope of the repulsive wall.

In 1982, Clary²¹ provided the first PES taking into account the symmetric and asymmetric stretch and the bending normal vibrational mode. Based on this surface computed with the SCF method, vibrational relaxation rate coefficients

for the 50 - 373 K temperature range were obtained with the VCC-IOS approach.

With increasing quality of experimental collisional data along the years, new and improved (semi)empirical PESs were provided, such as the 2-dimensional ones of Keil *et al.*^{22,23} and of Beneventi *et al.*²⁴ which were obtained by simultaneous analysis of different scattering properties.

In 1994, Weida *et al.*²⁵ provided the very first infra-red spectra of the CO₂-He vdW complex, and thus, a strong validation criteria for the PESs. It was recorded in the region of the ν_3 asymmetric stretch on the ¹²C¹⁶O₂ isotopologue. Later, Xu & Jäger²⁶ and McKellar²⁷ studies were also devoted to experimental spectra of this system. Xu & Jäger²⁶ reported an experimental spectra of pure rotational transitions for seven CO₂ isotopologues, including ¹²C¹⁶O₂, ¹³C¹⁶O₂, ¹²C¹⁸O₂ and ¹³C¹⁸O₂. McKellar²⁷ presented an experimental infra-red spectra obtained on 3 CO₂ isotopologues in the ν_3 band, including ¹³C¹⁶O₂ and ¹³C¹⁸O₂.

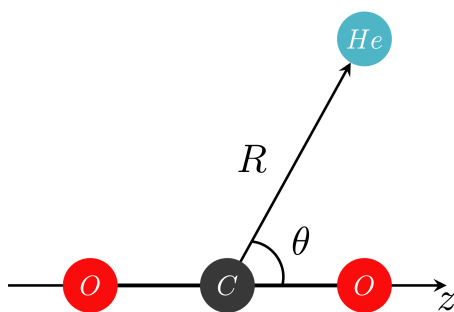
In order to interpret the recently obtained IR spectra, new PESs were established, as the one of Yan *et al.*²⁸ in 1998 and the one of Negri *et al.*²⁹ in 1999. Both these surfaces were computed using the fourth-order Møller-Plesset (MP4) perturbational theory with a large basis set containing mid-bond functions.

The so-called mid-bond functions are functions centered at half distance of the vdW bond, i.e. between the molecule and the rare gas atom. Such functions are often used since it has been shown to improve the accuracy of the potential well when limited basis sets are used. However, these orbitals have no physical meaning, and thus, it can also introduce an overestimation of the interaction energy in some regions of the PES.⁹

In Thibault *et al.*¹⁰ work, experimental pressure broadening coefficients were provided for various R and Q spectroscopic lines in the 123 - 760 K temperature range. They also computed such coefficients using the PESs of Negri *et al.*²⁹ Beneventi *et al.*²⁴ and Yan *et al.*²⁸ in order to evaluate the quality of these PESs. After running scattering calculations with the CC and the coupled-state (CS) approaches, they deduced that the PES of Negri *et al.*²⁹ was the most accurate of the three.

In 2001, Korona *et al.*³⁰ published a new PES computed with a symmetry-adapted perturbational theory (SAPT). The CO₂ molecule was considered as a rigid rotor and its bond length was set to 2.1944 a_0 . The rovibrational energy levels computed from variational calculations on their SAPT potential lead to an excellent agreement with experimental data of Weida *et al.*²⁵ indicating that the potential well is well described. The pressure broadening coefficients that they obtained with scattering calculations are also in the experimental error bars of Boissonles *et al.*³¹ and Thibault *et al.*¹⁰ measurements, suggesting the great quality of this PES.

Li & Le Roy³² and Ran & Xie⁸ included the effect of the antisymmetric-stretch Q_3 normal mode in the 3D-PESs that they computed with the CCSD(T) method in conjunction with an aVQZ basis set and additional mid-bond functions. Potential wells of both surfaces were validated through comparison between computed spectroscopic values and experi-

FIG. 1. CO₂-He collisional system in Jacobi coordinates.

mental measurements.

In 2009, two additional CO₂-He studies came out. Deng *et al.*¹¹ provided new experimental pressure broadening coefficients for the R(10) and P(2) lines in the ν_3 band at several temperature between 100 and 300 K. They compared them to the ones they obtained by scattering calculations performed on Korona *et al.*³⁰ PES. These coefficients were found between experimental error bars for almost all temperatures, which prove the accuracy of the repulsive wall on Korona *et al.*³⁰ PES. Yang & Stancil⁷ provided relaxation cross sections and quenching rate coefficients for rotational levels $j = 2, 4, 6, 8$ in the temperature range from 10^{-5} K up to 3000 K using Ran & Xie⁸ PES.

Two years later, al-Qady *et al.*¹³ published a study of cold collisions of highly rotationally excited CO₂ with helium. Based on Ran & Xie⁸ PES with a mix of the CC and the CS approaches, they computed cross sections for j up to 200.

Recently, Selim *et al.*³³ presented a new computational method to compute state-to-state rate coefficients of rovibrational transitions within this vdW complex. It is based on the CC approach for rotational transitions, and a multi-channel distorted-wave Born approximation for vibrational ones. They computed an *ab initio* three-dimensional PES, including Q_1 and Q_3 , the normal modes corresponding respectively to the symmetric and asymmetric CO₂ stretching ν_1 and ν_3 . They used a CCSD(T) method and an aVQZ basis with additional mid-bond functions.

III. METHODS

A. *ab initio* calculations

CO₂ is considered here as a rigid rotor. Its internuclear C — O distance is taken at $2.1944a_0$, the experimental average length over the ground vibrational wavefunction.³⁴ The interaction potential between CO₂ and He was described using Jacobi coordinates (R, θ) as presented in Figure 1.

The major attractive contribution to the PES in rare-gas-neutral-molecule complexes are dispersion energies.^{28,29} Hence, correlated method and large basis set must be used to compute the intermolecular interaction of such systems.³⁵ The PES was thus calculated using the CCSD(T) method with an empirical extrapolation to the complete basis set

(CBS) limit. This extrapolation is based on calculations using augmented correlation-consistent X zeta basis set (hereafter aVXZ), where $X = T, Q$, and 5. Thus, the basis is noted CBS(T,Q,5). The extrapolated energy E_{CBS} is obtained by solving the following set of equations:³⁶

$$E_X = E_{CBS} + Ae^{-(X-1)} + Be^{-(X-1)^2} \quad (1)$$

where A , and B are adjustable fitting parameters.

The basis set superposition error was corrected at every geometries (R, θ) with the counterpoise procedure of Boys & Bernardi:³⁷

$$V(R, \theta) = E_{CO_2-He}(R, \theta) - E_{CO_2}(R, \theta) - E_{He}(R, \theta) \quad (2)$$

where $V(R, \theta)$ is the interaction potential, and all energies E are computed with full basis set.

Calculations have been performed for $R \in [4, 20]a_0$ with a step depending on the short/intermediate/long range regions of interactions, and for $\theta \in [0, 90]^\circ$ with a regular step of 10° . In total, 260 *ab initio* points were calculated with the MOLPRO software.³⁸

A global fit of the potential was performed using an expansion over Legendre polynomials $P_\lambda(\cos\theta)$.³⁹

$$V(R, \theta) = \sum_{\lambda=0}^{\lambda_{max}} v_\lambda(R) P_\lambda(\cos\theta) \quad (3)$$

where λ_{max} was taken equal to 18 according to the numbers of θ angles chosen for the *ab initio* calculations. In fact, given the CO₂ symmetry, only even Legendre polynomials appear in the sum. The radial coefficients $v_\lambda(R)$ have been fitted as:³⁹

$$v_\lambda(R) = e^{-a_1^\lambda R} (a_2^\lambda + a_3^\lambda R + a_4^\lambda R^2 + a_5^\lambda R^3) - \frac{1}{2} [1 + \tanh R/R_{ref}] \left(\frac{C_6^\lambda}{R^6} + \frac{C_8^\lambda}{R^8} + \frac{C_{10}^\lambda}{R^{10}} \right) \quad (4)$$

where a_n^λ are the expansion coefficients, and the coefficients of the R^{-n} terms are symbolized by C_n^λ . The latter are then used for the long-range extrapolation. The hyperbolic tangent factor provided a smooth transition between the short-range ($0 < R < R_{ref}$) and the long-range regions ($R > R_{ref}$). The fitted potential reproduces all of our *ab initio* points with an error inferior to 1%. The root-mean-square error of the fitted potential is of 0.0149 cm^{-1} , and is mostly due to deviation at short distances.

In Fig. 2, we compare the long-range of interactions of our PES to the one of Li & Le Roy.³² The latter used a multipolar expansion to determine the C_n^λ coefficients so their long-range of interactions is trustworthy. The agreement is excellent over the full range of angles and distances presented here, so we can be confident in the accuracy of our PES for low temperature collisions.

B. Bound states calculations

Bound states were computed in the ground vibrational state with the BOUND software.⁴⁰ Calculations were per-

Sample title

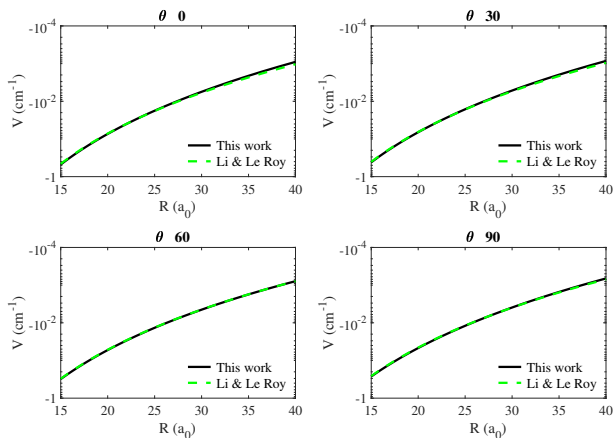


FIG. 2. Comparison(s) of the long-range of interactions of our and Li & Le Roy³² PESs for $\theta = 0, 30, 60$ and 90° .

formed with the CC approach. The coupled equations were solved with the log-derivative method of Manolopoulos.⁴¹ The propagation step was set to $0.01a_0$, the rotational basis included the first 16 rotational levels (up to $j = 30$ since only rotational levels with even j exists due to nuclear spin statistics) and the maximum distance of propagation was set at $30a_0$. These parameters were converged in order to get an error lower than 0.001% on bound state energies.

Transition frequencies were computed for the different carbon dioxide isotopologues: $^{12}\text{C}^{16}\text{O}_2$, $^{13}\text{C}^{16}\text{O}_2$, $^{12}\text{C}^{18}\text{O}_2$ and $^{13}\text{C}^{18}\text{O}_2$. Their respective rotational constants were set at $B_0 = 0.390219$; 0.390237 ; 0.346817 and 0.346834 cm^{-1} .^{25,42,43}

C. Scattering calculations

As introduced earlier, CO_2 is an interesting molecule for cometary and planetary atmospheres, ISM and protoplanetary disks. Such media generally exhibit temperature between 10 and 300 K.^{2,3,44} At 300 K, assuming a Boltzmann distribution of the population on the energy levels, levels with internal energy lower than 500 cm^{-1} can be significantly populated. Hence, we performed scattering calculations for rotational levels up to $j = 40$ which corresponds to over 96% of the population assuming a Maxwell-Boltzmann distribution over the rotational energy levels.

In order to ensure the accuracy of our results up to this j for this temperature range, calculations were carried out for a range of total energy E from 2.4 cm^{-1} up to 2500 cm^{-1} . The grid of energy is really dense at low energies to correctly describe resonances and, as the energy increases, the energy step also increases.

The scattering matrix, also called the S-matrix, is obtained through a CC approach with the log-derivative method of Manolopoulos⁴¹ implemented in the MOLSCAT program.⁴⁵

Propagation parameters and maximum total angular momentum J_{max} were automatically converged by the

$E \text{ (cm}^{-1}\text{)}$	j_{max}	J_{max}	STEPS	λ_{max}	DNRG
2.4 - 10	12	12 - 17	74	14	0.1
10 - 20	12	17 - 21	74	14	0.2
20 - 50	16	21 - 28	24	14	0.2
50 - 100	20	28 - 36	19	14	0.2
100 - 150	24	36 - 41	15	14	0.2
150 - 200	28	41 - 45	13	14	0.5
200 - 300	32	45 - 53	12	18	0.5
300 - 500	40	53 - 65	22	18	1
500 - 1000	54	65 - 84	10	16	2
1000 - 2500	54	84 - 117	6	14	50

TABLE I. MOLSCAT parameters j_{max} , J_{max} , λ_{max} , STEPS depending of the energy, and the energy step DNRG used to span the energy grid.

MOLSCAT code. The rotational basis set fixed by j_{max} the rotational quantum number of CO_2 , the number of Legendre polynomials used, fixed by λ_{max} and the STEPS of propagation were set after series of convergence tests in order to ensure the convergence of the S-matrix over all the energy interval considered with an error lower than 1%. These parameters are presented in Table I.

1. Rate coefficients

From the S-matrix, noted $S^J(j'l', jl)$ hereafter, with J the total angular momentum quantum number, l and j the relative angular and rotational quantum numbers, state-to-state cross sections $\sigma_{j'l' \leftarrow j}$ are obtained as:⁴⁶

$$\sigma_{j'l' \leftarrow j} = \frac{\pi}{(2j+1)k_j^2} \sum_{J=0}^{\infty} \sum_{l=|J-j|}^{J+j} \sum_{l'=|J-j'|}^{J+j'} (2J+1) \times \delta_{jj'} \delta_{ll'} - |S^J(j'l', jl)|^2 \quad (5)$$

with the squared wavenumber $k_j^2 = \frac{2\mu}{\hbar^2} [E - E_j]$, where E is the total energy of the system, and E_j is the energy of the j^{th} rotational level of the rigid rotor.

Rate coefficients $k_{j'l' \leftarrow j}$ are Maxwellian average of these collisional cross sections at a given temperature T such as:⁴⁶

$$k_{j'l' \leftarrow j}(T) = \sqrt{\frac{8k_B T}{\pi\mu}} \left(\frac{1}{k_B T} \right)^2 \times \int_0^{\infty} E_{kin} \sigma_{j'l' \leftarrow j}(E_{kin}) e^{-(E_{kin}/k_B T)} dE_{kin} \quad (6)$$

where k_B is the Boltzmann constant, and $E_{kin} = E - E_j$ the kinetic energy of the collision.

2. Pressure broadening (PB) coefficients

PB coefficients, which are by-products of S-matrices, were computed for the R(0), R(10) and P(2) lines corresponding to the v_3 band ($00^00 \rightarrow 00^01$).

Only rotational levels with even values of j exist in the vibrational ground state (00^00), and only the ones with odd j values exist in v_3 (00^01) due to nuclear spins statistics.²⁷ Since our PES was computed only for the ground vibrational state, we made the assumption that both these vibrational states have the same PES which means that we neglected the vibrational dependence of the PES. In addition, the vibrational coupling was also neglected and thus, it is equivalent to consider all rotational states, with even and odd j , on the same PES.

PB coefficients γ^0 designate the *half-width-at-half-maximum* (HWHM) of the Lorentzian-shape spectroscopic line. Its normalized per helium atmosphere expression is:^{10,30}

$$\gamma^0 = n_p \bar{v} \langle \sigma^{(n)}(jj'; E_{kin}) \rangle = \frac{56.6915}{\sqrt{\mu T}} \bar{\sigma} \quad (7)$$

where γ^0 unit is $10^{-3} \text{ cm}^{-1} \text{ atm}^{-1}$, n_p is the density of perturbers, $\bar{v} = \sqrt{(8k_B T / \pi \mu)}$ is the mean velocity, μ is the reduced mass of the $\text{CO}_2\text{-He}$ complex, and $\bar{\sigma}$ is the thermally averaged PB cross sections in \AA^2 . These PB cross sections are expressed as follow:¹⁰

$$\begin{aligned} \sigma^{(n)}(jj'; E_{kin}) &= \left(\frac{\pi}{k_j^2} \right) \sum_{JJ'l'} (2J+1)(2J'+1) \\ &\times \left\{ \begin{matrix} j & n & j' \\ J' & l & J \end{matrix} \right\} \left\{ \begin{matrix} j & n & j' \\ J' & l' & J \end{matrix} \right\} \left[\delta_{ll'} - \langle j'l' | S^J(E_{kin} + E_j) | jl \rangle \right. \\ &\quad \left. \times \langle j'l' | S^{J'}(E_{kin} + E_{j'}) | j'l \rangle^* \right] \end{aligned} \quad (8)$$

where n is the tensor order of the radiative transition ($0 =$ isotropic Raman, $1 =$ infrared, $2 =$ anisotropic Raman).

IV. PES

Our PES, computed at the CCSD(T)/CBS(T,Q,5) level of theory, has a global minimum $V = -49.22 \text{ cm}^{-1}$ for the T-shape complex ($\theta = 90^\circ$) at $R = 5.78a_0$, and a local minimum $V = -26.51 \text{ cm}^{-1}$ for the linear geometry ($\theta = 0^\circ$) at $R = 8.05a_0$. A representation of this PES is given in 3D in Fig. 3, and its isocontours are presented in Fig. 4.

Our PES is compared to some of the most recently published, of Negri *et al.*,²⁹ Korona *et al.*,³⁰ Ran & Xie,⁸ and Li & LeRoy³² in Table II that exhibits positions and well depths of the global and local minima. In present and previous studies, minima are at the same geometry (T-shape and linear-shape).

As found in previous studies, the interaction around the global minimum is highly anisotropic. Positions and well depths of all PESs are in really good agreement. Negri *et al.*²⁹ PES, has the least deep potential wells, followed by ours. The potential wells obtained by Korona *et al.*,³⁰ for both the T-shape and the linear-shape complex are the deepest ones.

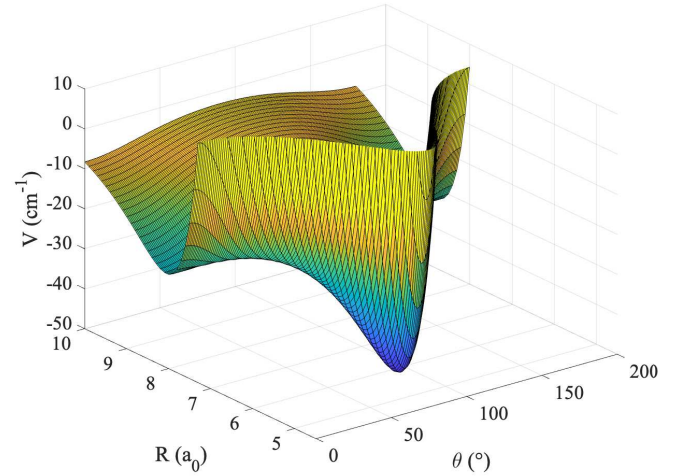


FIG. 3. PES in 3D of the $\text{CO}_2\text{-He}$ collisional system.

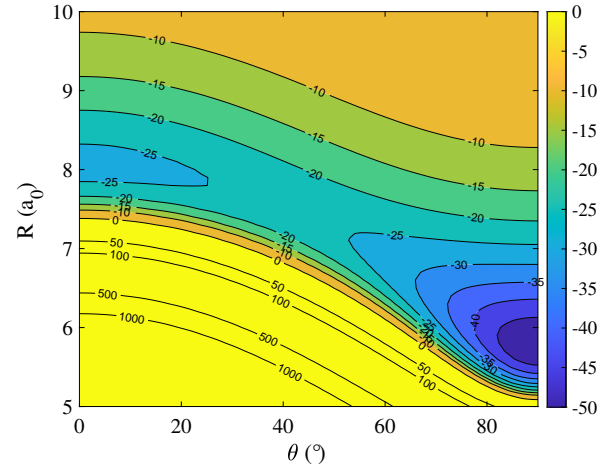


FIG. 4. Isocontours of the PES of the $\text{CO}_2\text{-He}$ collisional system.

TABLE II. Properties of global ($\theta = 90^\circ$) and local ($\theta = 0^\circ$) minima for present and previously computed PESs of the $\text{CO}_2\text{-He}$ vdW complex.

Reference	Global minimum		Local minimum	
	R (a_0)	V (cm^{-1})	R (a_0)	V (cm^{-1})
This work	5.78	-49.22	8.05	-26.51
Negri <i>et al.</i> ²⁹	5.86	-45.98	8.13	-26.31
Korona <i>et al.</i> ³⁰	5.81	-50.38	8.03	-28.94
Ran & Xie ⁸	5.79	-49.39	8.06	-26.70
Li & LeRoy ³²	5.78	-49.57	8.06	-26.69

Their global minimum is over 2% deeper than our, and almost 10% deeper than Negri *et al.*²⁹ minima. Ran & Xie,⁸ Li & LeRoy³² and us have very similar PESs, which is not surprising since we used a similar theoretical approach.

Sample title

As we did not use any midbond functions, and used a highly correlated method with an extrapolation to the complete basis set, we are confident in the accuracy of our PES for the short, intermediate and long range of interactions. It will be demonstrated by comparison between theoretical data computed based on our PES and experimental measurements such as bound state transition frequencies and pressure broadening coefficients.

V. TEST OF THE NEW CO₂-HE PES ACCURACY

A. Bound states

We have computed the energies of the bound states supported by the CO₂-He vdW well. The transition frequencies in the CO₂-He complex were deduced from the computed bound state energies. Frequencies of $\Delta(0_{00} - 1_{01})$, $\Delta(0_{00} - 1_{11})$, $\Delta(0_{00} - 2_{02})$ and $\Delta(0_{00} - 3_{03})$ transitions were computed for 4 CO₂ isotopologues: ¹²C¹⁶O₂, ¹³C¹⁶O₂, ¹²C¹⁸O₂ and ¹³C¹⁸O₂. Bound states are labeled with the rigid asymmetric rotor quantum numbers $J_{K_a K_c}$, where K_a and K_c are projections of J over inertia moments axis. Our frequencies and previous theoretical ones from Korona *et al.*,³⁰ Li & LeRoy,³² and Ran & Xie⁸ are presented in Table III. This Table contains also the absolute relative error = $|v_{th.} - v_{exp.}|/v_{exp.}$ with experimental values, which come from Xu & Jäger²⁶ for ¹²C isotopologues, and from McKellar²⁷ for ¹³C ones.

Computed frequencies of the $\Delta(0_{00} - 1_{01})$ transition for the ¹²C¹⁶O₂ isotopologue are very similar for all theoretical studies^{8,30,32} and in good agreement with the experimental measurement, the relative errors being lower than 0.6%. Additionally, Li & LeRoy³² and us computed other transition frequencies, as the $\Delta(0_{00} - 1_{01})$ one for the ¹³C¹⁶O₂ isotopologue, and the $\Delta(0_{00} - 1_{11})$ for both ¹²C¹⁸O₂ and ¹³C¹⁸O₂ isotopologues. Again, results are similar and in excellent agreement with experimental values. We also provide further transition frequencies, $\Delta(0_{00} - 2_{02})$ and $\Delta(0_{00} - 3_{03})$ for ¹³C-based isotopologues. They are in very good agreement with experimental values, the highest absolute error for these transitions being $\sim 0.3\%$. Thus, the accuracy of the shape and the depth of the potential well is validated.

B. Pressure broadening coefficients

The PB coefficients that we obtained with our PES for the ¹²C¹⁶O₂ isotopologue were compared to experimental ones provided by Thibault *et al.*¹⁰ and Deng *et al.*¹¹ in Fig. 5. The later made their measurements with the ¹³CO₂ isotopologue and indicated that the substitution of ¹²CO₂ by ¹³CO₂ includes an error smaller than 0.1% on calculated PB cross sections.¹¹ Our results are also compared to theoretical ones provided by Deng *et al.*¹¹ for the R(10) and P(2) lines, and by Korona *et al.*³⁰ for the R(0) line. Both these calculations were performed based on Korona *et al.*³⁰ PES.

As expected from Eq. (7) (in particular at room temperature), the HWHM for all considered lines are decreasing

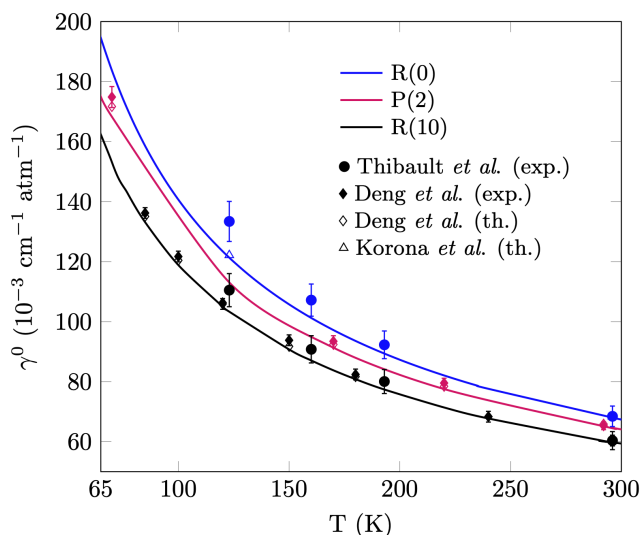


FIG. 5. HWHM γ^0 for R(0), R(10) and P(2) lines from our theoretical study (lines); experimental studies of Thibault *et al.*¹⁰ (●) and Deng *et al.*¹¹ (◆); theoretical results of Deng *et al.*¹¹ (◇) and Korona *et al.*³⁰ (△); both obtained using Korona *et al.*³⁰ PES. The marks are color coded for the lines investigated. Some of the experimental values overlay theoretical ones.

with increasing temperature. Our results as these theoretically obtained based on Korona *et al.*³⁰ PES show an overall good agreement with experimental measurements for all the present lines. At lower temperature, the agreement is slightly less good with Thibault *et al.*¹⁰ data but they pointed out that their experimental values for this temperature range may suffer of an unexplained bias.¹⁰ However, at temperature above 200 K our results are within the error bars, indicating that the accuracy of the PES is good. In addition, we note that both the experimental set up and the lineshape analysis used by Deng *et al.*¹¹ are more accurate than the ones used by Thibault *et al.*¹⁰ Thus the very good agreement between our calculated values for the P(2) and R(10) HWHM, and Deng *et al.*¹¹ experimental results gives us confidence in the quality of our PES.

The temperature range investigated is above the dissociation limit of the bound complex, and thus, this comparison with experimental data is mainly a test of the repulsive wall.¹¹ Therefore, the repulsive wall of our surface is validated.

VI. COLLISIONAL DATA & DISCUSSION

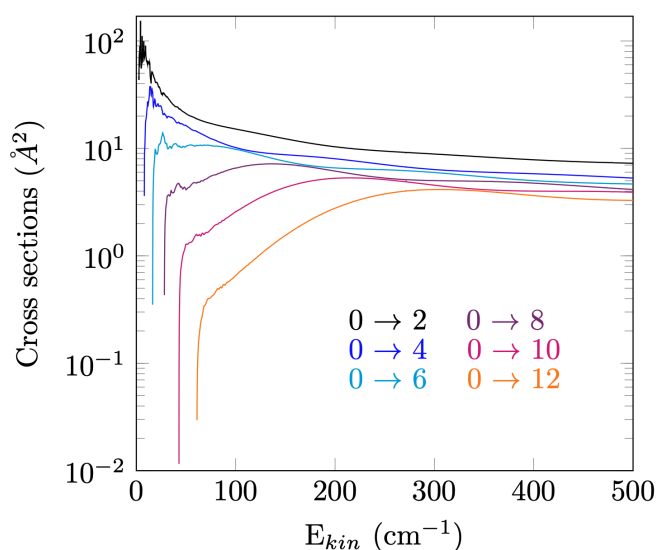
A. Inelastic cross sections and rate coefficients

In Figure 6, cross sections resulting from scattering calculations detailed in III.C, are provided for excitations from the rotational level $j = 0$ for various $\Delta j = |j' - j|$ as a function of the kinetic energy.

At low collisional energy ($E_{kin} \sim 50 \text{ cm}^{-1}$), Feshbach and shape resonances⁴⁷ can be observed. They are due to a

TABLE III. Frequencies of several bound state transitions within ν_0 for different isotopologues and theoretical studies.^{8,30,32}

$\Delta(J_{K_a K_c} - J'_{K'_a K'_c})$	Isotopologues		This work	Ran & Xie ⁸	Korona <i>et al.</i> ³⁰	Li & LeRoy ³²
$\Delta(0_{00} - 1_{01})$	¹² C ¹⁶ O ₂	ν (cm ⁻¹)	0.589	0.589	0.592	0.588
		abs. error (%) ²⁶	0.436	0.436	0.072	0.588
	¹³ C ¹⁶ O ₂	ν (cm ⁻¹)	0.588			0.587
		abs. error (%) ²⁷	0.508			0.677
$\Delta(0_{00} - 1_{11})$	¹² C ¹⁸ O ₂	ν (cm ⁻¹)	0.576			0.575
		abs. error (%) ²⁶	0.472			0.645
	¹³ C ¹⁸ O ₂	ν (cm ⁻¹)	0.575			0.575
		abs. error (%) ²⁷	0.519			0.519
$\Delta(0_{00} - 2_{02})$	¹³ C ¹⁶ O ₂	ν (cm ⁻¹)	1.577			
		abs. error (%) ²⁷	0.316			
	¹³ C ¹⁸ O ₂	ν (cm ⁻¹)	1.482			
		abs. error (%) ²⁷	0.202			
$\Delta(0_{00} - 3_{03})$	¹³ C ¹⁶ O ₂	ν (cm ⁻¹)	2.919			
		abs. error (%) ²⁷	0.311			

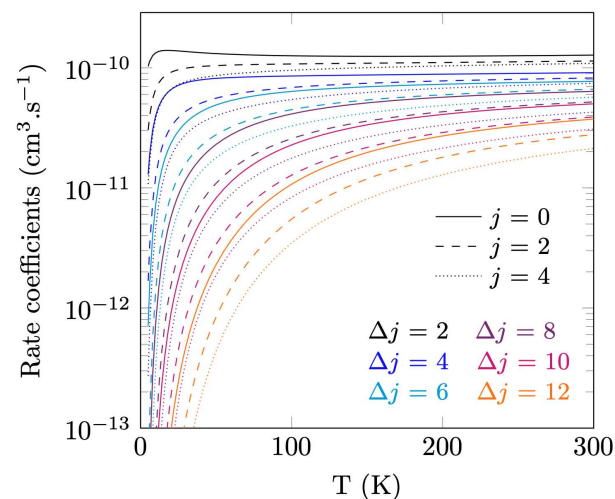
FIG. 6. Cross sections for $j = 0$ at various Δj as a function of kinetic energy.

temporary formation of the CO₂-He vdW complex when the energy corresponds to a (quasi)bound state energy in the potential well. It explains why such resonances disappear when kinetic energy is large compare to the well depth. Thus, in order to correctly represent such phenomena, the grid of energy needs to be really dense at low energy.

The general propensity rule is, as expected, favouring excitation with the lowest Δj (here equal to 2 since rotational levels with odd j do not exist), in agreement with the exponential energy-gap behavior.⁷ So as Δj increases, so does the energy-gap, and thus cross sections decrease. However, for cross sections with a $\Delta j \geq 6$, this propensity rule vanishes at particular collisional energy, and cross sections for this Δj is similar to cross sections for $\Delta j \pm 2$. For example,

$\sigma_{0 \rightarrow 4} \sim \sigma_{0 \rightarrow 6}$ at $E_{kin} \sim 110$ cm⁻¹, $\sigma_{0 \rightarrow 6} \sim \sigma_{0 \rightarrow 8}$ at $E_{kin} \sim 170$ cm⁻¹ and $\sigma_{0 \rightarrow 8}$ is also similar to $\sigma_{0 \rightarrow 10}$ at $E_{kin} \sim 240$ cm⁻¹. It is also the case for $\sigma_{0 \rightarrow 10}$ which is almost equal to $\sigma_{0 \rightarrow 12}$ at $E_{kin} \sim 340$ cm⁻¹. The small difference between the cross sections at higher kinetic energies can be explained by the fact that the rotational constant of the CO₂ molecule is low, and thus, the energy spacing between rotational states becomes negligible compared to the kinetic energy.

Rate coefficients presented in Fig. 7 were obtained from thermal averaging of the above state-to-state cross-sections.

FIG. 7. Excitation rate coefficients from $j = 0, 2, 4$ for various Δj as a function of temperature.

The propensity rule is still favouring (de-)excitation with the lowest Δj . These rate coefficients decrease as the initial rotational quantum number j increases because of the increasing energy gap to reach next levels. However, contrary to cross sections of Fig. 6, this rule does not vanish over the

temperature range explored in this work. It is explained by the high weight given to low kinetic energy behavior in the Maxwellian average of the cross sections. In addition, we can observe that an asymptotical value is reached for rate coefficients with $\Delta j \leq 6$.

In order to observe the sensitivity of the rate coefficients to the PES, our relaxation rate coefficients from $j = 8$ to $j' = 6, 4, 2$, and 0 are compared in Figure 8 to the ones of Yang & Stancil⁷ which were computed on Ran & Xie⁸ PES. Their dynamical calculations were performed with the CC approach for collisional energies lower than 500 cm^{-1} and with the CS approximation for energies up to 10^4 cm^{-1} . The looked up rotational level here is $j = 8$, which states at 28.096 cm^{-1} , and thus, we consider that we are comparing here rate coefficients obtained with very similar dynamical calculations and then, that the observed differences will be due almost exclusively to the different PESs used.

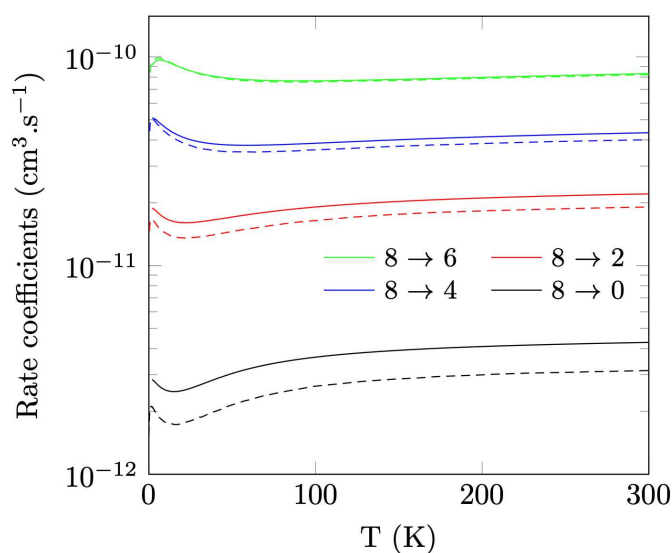


FIG. 8. Relaxation rate coefficients from Yang & Stancil⁷ (- -) and our (-) study for $j = 0, 2, 4$ for various j' as a function of temperature.

Our rate coefficients (solid lines) and the ones of Yang & Stancil⁷ (dashed lines) have the same behavior, and the agreement for low Δj is very good. However, for larger Δj transitions, the new rate coefficients can be 1.5 times larger than the former ones. In fact, the bigger Δj is, the larger the difference is.

In the present case, we can suspect that their radial coefficients for $l \geq 6$ are smaller than ours (v_8 in particular), a consequence of a slightly lower anisotropy of their PES. In this temperature range, the rate coefficients are more sensitive to the short/intermediate-range of interaction on the PES. Thus, it is the anisotropy in the PES well and on the repulsive wall that must differ and leads to non-negligible differences in the scattering calculations.

Despite the use of similar approaches and *ab initio* methods leading to a difference on the global minimum of the surface inferior to 1% and a similar dynamical method

(CC), the difference between the rate coefficients can be up to 50%. Indeed, the magnitude of the cross sections is determined by both the well depth and the global anisotropy of the PES. Therefore, it is a primary importance to use a PES as accurate as possible.

B. CO₂: a super-rotor in helium-buffer-gas

In the aim of checking the effect of different PESs on cross sections for this collisional system, we compared our cross sections to the ones of al-Qady *et al.*¹³ in Fig. 9. Our results are in solid lines, and theirs are in dashed lines.

The main purpose of al-Qady *et al.*¹³ study was the demonstration of the feasibility of producing CO₂ super-rotors, i.e. highly rotationally excited CO₂ in a cold helium-buffer-gas. Producing this kind of systems can be useful in order to study intramolecular forces, inelastic collisions and cold chemistry.¹³

To produce such a stable system, the elastic cross section of a rotational level j must be larger than the downward cross sections at the cryogenic temperature of the buffer-gas, which is 4.2 K in the case of helium at atmospheric pressure. To provide cross sections from $j = 10, 20, 24, 30$ and 40 , al-Qady *et al.*¹³ used Ran & Xie⁸ PES and performed CC scattering calculations.

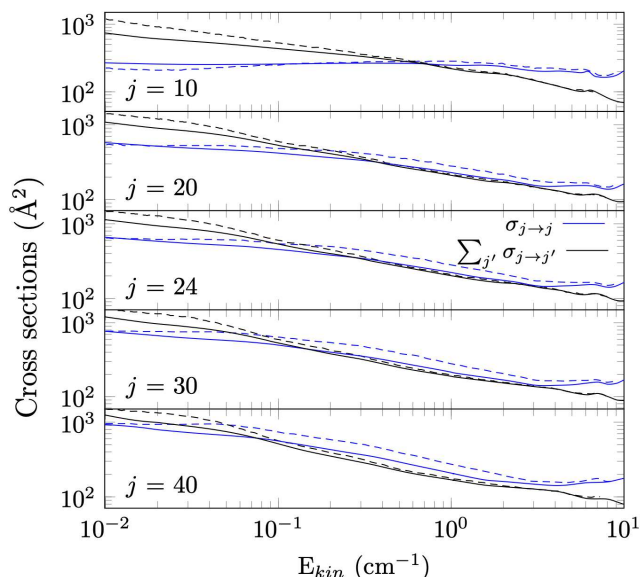


FIG. 9. Elastic (blue) and quenching (black) cross sections for CO₂ and He collisions at $j = 10, 20, 24, 30$ and 40 in al-Qady *et al.*¹³ (- -) and our (-) study.

The crossing between lines represents the physical conditions from which rotationally excited CO₂ is stable in a buffer-gas of helium despite collisions occur. Both studies give similar results, tendency and crossing energies. In both of them, we observe that, the higher the j is, the lower the kinetic energy is at the crossing between the lines so the wider is the temperature range of stability for the super-rotor. It suggests

that producing stable CO₂ super-rotor in a helium-buffer-gas is feasible.

However, the stability of such super-rotors may have been overestimated. In fact, our elastic cross sections are lower than the ones obtained by al-Qady *et al.*¹³ Furthermore, our crossing energies are slightly shifted to higher values of energy, indicating a decreasing stability of the system compared to the previous results. Therefore, stable CO₂ super-rotor in a helium-buffer-gas appears to be possible, even though a bit more difficult to generate than previously predicted.

Moreover, another point needs to be highlighted: there is up to almost 30% of difference on the quenching cross sections at low energy. It exhibits that, at low collisional energies, cross sections (and thus rate coefficients) are really sensitive to the PES. In their study, Yang & Stancil⁷ also emphasized this point by comparing state-to-state cross sections obtained with Negri *et al.*,²⁹ Korona *et al.*,³⁰ and Ran & Xie⁸ PESs for collisional energies between 5×10^{-4} and 100 cm^{-1} . They exhibited that even the behavior of these cross sections can be different depending on the PES used.

The potential well depth of both surfaces are really similar, and the repulsive wall is not a topological features of importance at such low collisional energy,²² contrary to the long-range of interactions. We can thus confirm that rotational inelastic cross sections are highly sensitive to the global anisotropy of the system (along all the radial coordinate), as suggested by Benveneti *et al.*,²⁴ and specifically to the anisotropy of the long-range of interactions in the present case.

VII. CONCLUSIONS

This work presented a new potential energy surface of the CO₂-He van der Waals complex. It was computed with the highly correlated CCSD(T) method and an extrapolation to the complete basis set, noted CBS(T, Q, 5). The PES accuracy was tested through a comparison between theoretical and experimental bound states transition frequencies and pressure broadening coefficients. The very good agreement with experimental results certified that the computed PES is homogeneously accurate.

After the validation of our PES, collisional cross sections, which exhibited characteristic resonances, were calculated with the CC approach. By Maxwellian average of these cross sections, revised rate coefficients for this system in the 10 - 300 K temperature range were obtained.

Our rate coefficients exhibit up to 50% differences with the ones computed by Yang & Stancil⁷ based on Ran & Xie⁸ PES, even though a similar dynamical approach was used. Based on this same PES and with the same dynamical approach, al-Qady *et al.*¹³ computed cross sections at low temperature which are found up to 30% lower than ours. It was thus highlighted that small discrepancies on the short and long-range anisotropy of the PES can induce significant differences on collisional data, which need to be as accurate as possible for astrophysical modeling.

CO₂-He rate coefficients can be used as a first approximation⁵ to model more complex CO₂-bearing collisional systems, such as CO₂-H₂ or CO₂-H which are useful systems for interstellar molecular clouds and planetary atmospheres. Knowing that the new rates can be up to 1.5 bigger than the old ones suggest that the use of improved scattering data can lead to non-negligible consequences on the modeling of the CO₂ abundance in a large variety of astrophysical media. In addition, measuring the CO₂ abundances is also a test of astrochemical models, since this molecule is at the end of reaction chains, implying the CO molecule and the OH radical, or the O₂ molecule and CH₂ or HCCO.⁴⁸

ACKNOWLEDGEMENTS

We acknowledge financial support from the European Research Council (Consolidator Grant COLLEXISM, Grant Agreement No. 811363) and the Programme National “Physique et Chimie du Milieu Interstellaire” (PCMI) of CNRS/INSU with INC/INP cofunded by CEA and CNES.

F.L. acknowledges the Institut Universitaire de France.

A.G. acknowledges B. Desrousseaux, C. Bop, S. Demes and M. Żóttowski for their help and support during this work.

CONFLICTS OF INTEREST

The authors have no conflicts to disclose.

SUPPLEMENTARY MATERIAL

A Fortran subroutine of the potential energy surface is available as the supplementary material.

DATA AVAILABILITY

The data that support the findings of this study are available from the corresponding author upon reasonable request.

¹L. D’Hendecourt and M. Jourdain de Muizon, **223**, L5 (1989).

²A. D. Bosman, S. Bruderer, and E. F. van Dishoeck, **601**, A36 (2017).

³D. Despois, N. Biver, D. Bockelée-Morvan, and J. Crovisier, Proceedings of the International Astronomical Union **1**, 469 (2006).

⁴E. F. van Dishoeck, Annual Review of Astronomy and Astrophysics **42**, 119 (2004).

⁵E. Roueff and F. Lique, Chemical Reviews **113**, 8906 (2013).

⁶J. Cernicharo, J. R. Goicoechea, and E. Caux, **534**, 4 (2000).

⁷B. Yang and P. C. Stancil, The Journal of Chemical Physics **130**, 134319 (2009).

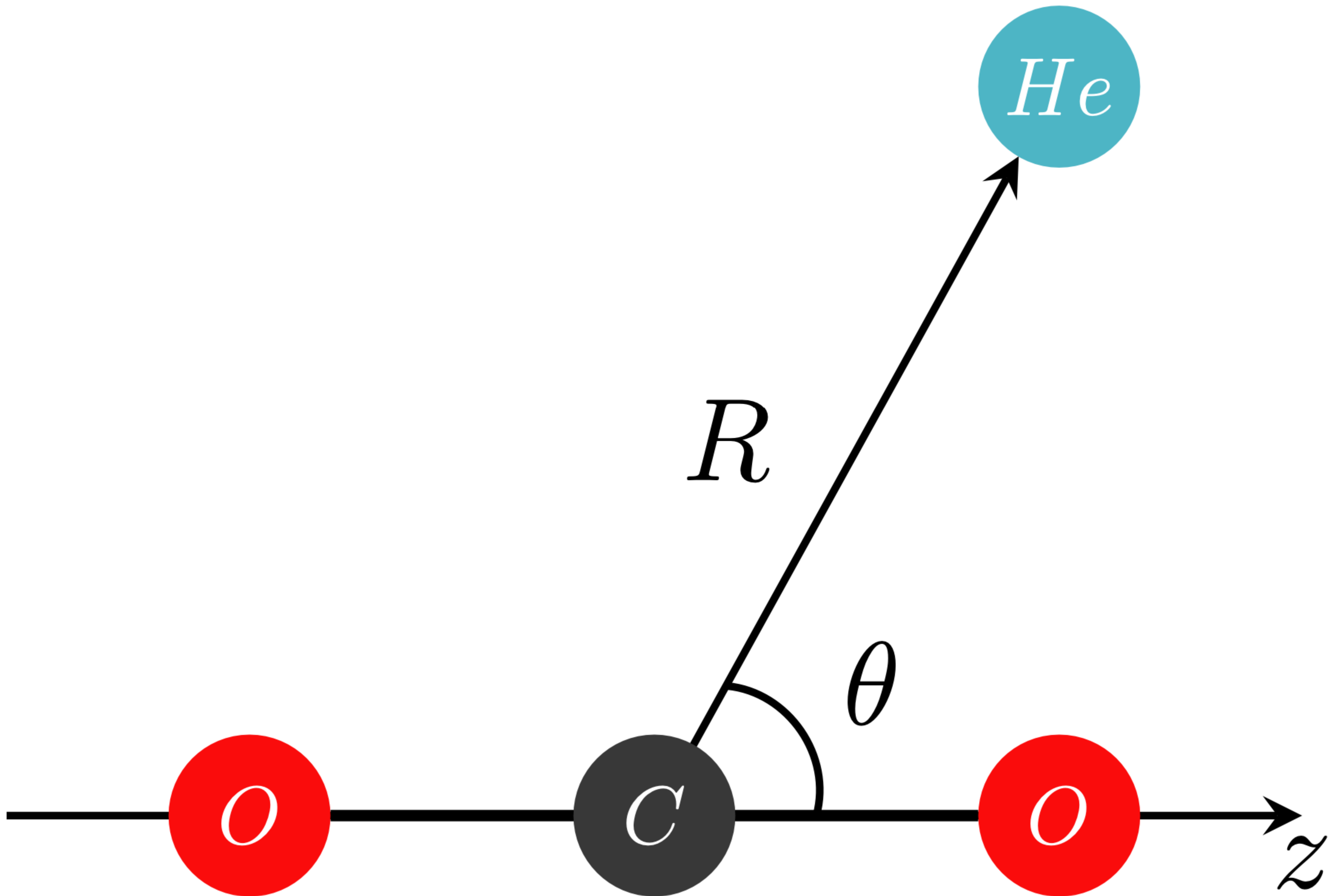
⁸H. Ran and D. Xie, The Journal of Chemical Physics **128**, 124323 (2008).

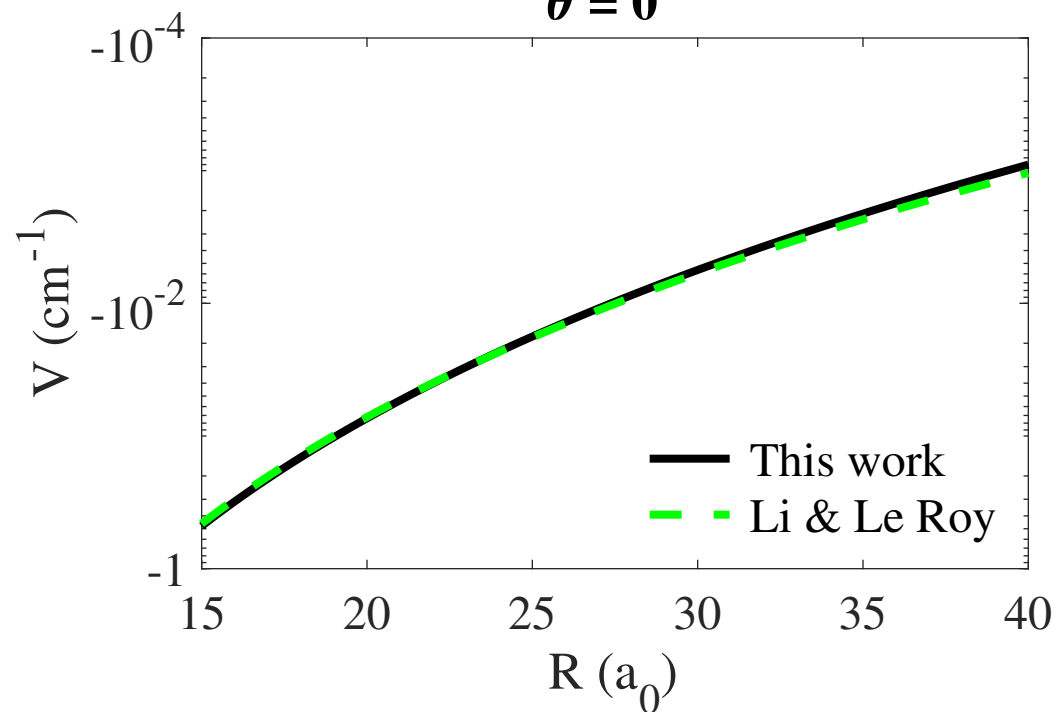
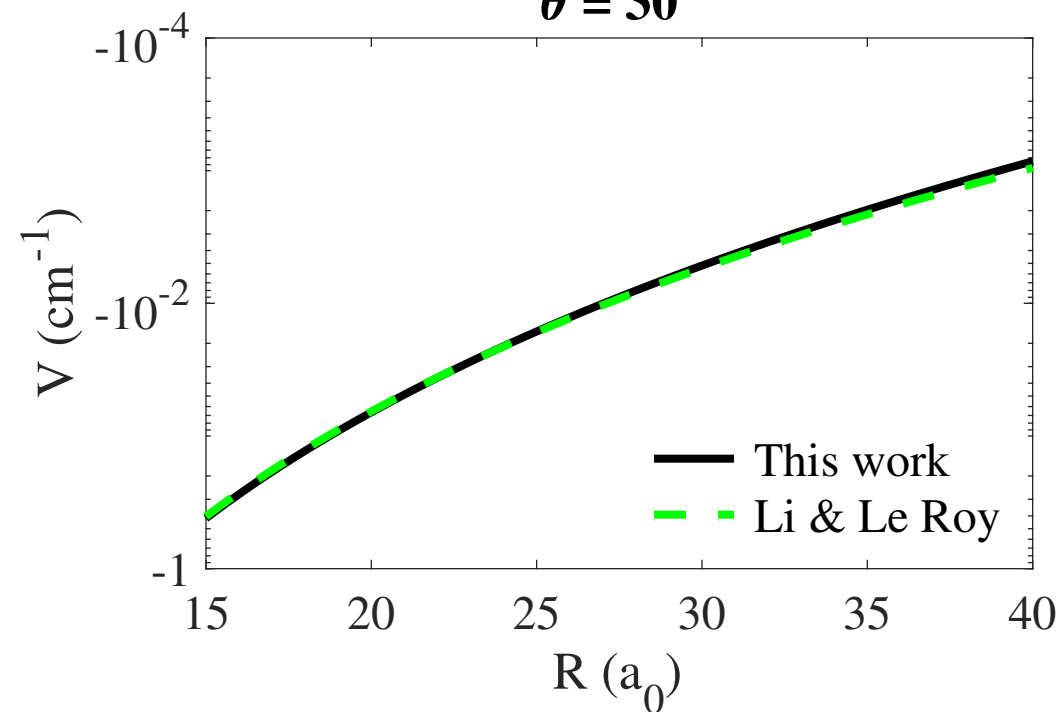
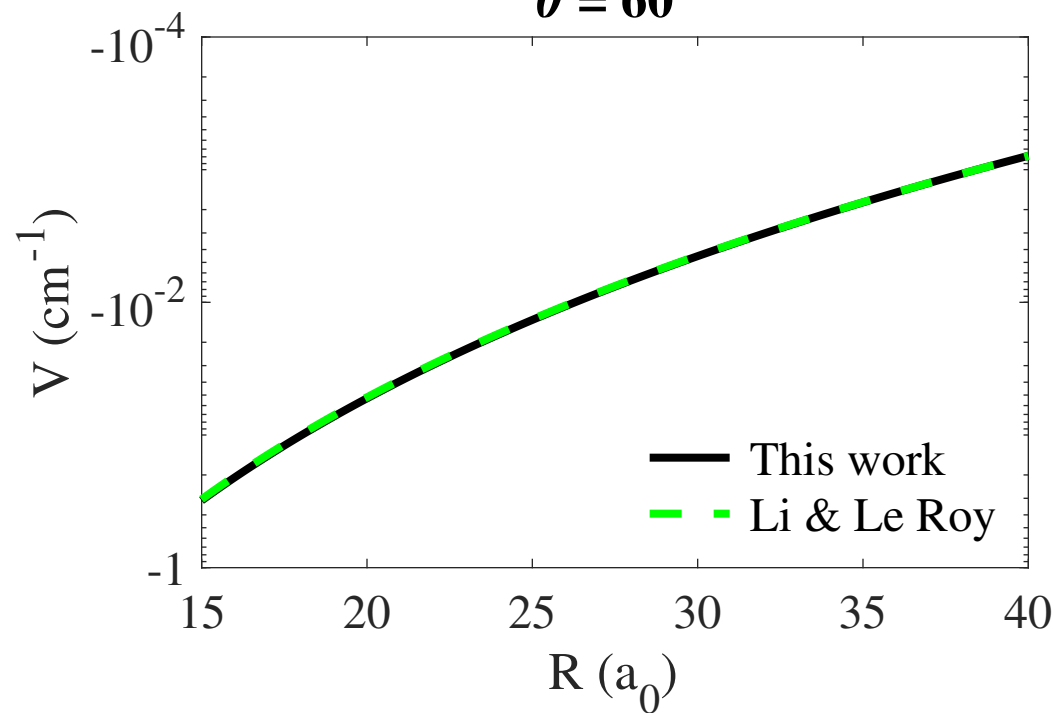
⁹R. Matveeva, M. Falck Erichsen, H. Koch, and I.-M. Høyvik, Journal of Computational Chemistry **43**, 121 (2021).

¹⁰F. Thibault, B. Calil, J. Boisssoles, and J. M. Launay, Physical Chemistry Chemical Physics **2**, 5404 (2000).

¹¹W. Deng, D. Mondelain, F. Thibault, C. Camy-Peyret, and A. W. Mantz, Journal of Molecular Spectroscopy **256**, 102 (2009).

- ¹²As it can be seen in Section II, all recent CO₂-He PES were computed with mid-bond functions so we wanted to provide the first highly accurate PES without them.
- ¹³W. H. al-Qady, R. C. Forrey, B. H. Yang, P. C. Stancil, and N. Balakrishnan, *Physical Review A* **84**, 054701 (2011).
- ¹⁴V. Nikulin and Y. Tsarev, *Chemical Physics* **10**, 433 (1975).
- ¹⁵R. G. Gordon and Y. S. Kim, *The Journal of Chemical Physics* **56**, 3122 (1972).
- ¹⁶Y. S. Kim and R. G. Gordon, *The Journal of Chemical Physics* **60**, 1842 (1974).
- ¹⁷G. A. Parker, R. L. Snow, and R. T. Pack, *The Journal of Chemical Physics* **64**, 1668 (1976).
- ¹⁸G. A. Parker and R. T. Pack, *The Journal of Chemical Physics* **68**, 1585 (1978).
- ¹⁹M. Keil, G. A. Parker, and A. Kuppermann, *Chemical Physics Letters* **59**, 6 (1978).
- ²⁰C. L. Stroud and L. M. Raff, *The Journal of Chemical Physics* **72**, 5479 (1980).
- ²¹D. Clary, *Chemical Physics* **65**, 247 (1982).
- ²²M. Keil and G. A. Parker, *The Journal of Chemical Physics* **82**, 1947 (1985).
- ²³M. Keil, L. J. Rawluk, and T. W. Dingle, *The Journal of Chemical Physics* **96**, 6621 (1992).
- ²⁴L. Beneventi, P. Casavecchia, F. Vecchiocattivi, G. G. Volpi, U. Buck, C. Lauenstein, and R. Schinke, *The Journal of Chemical Physics* **89**, 4671 (1988).
- ²⁵M. J. Weida, J. M. Sperhac, D. J. Nesbitt, and J. M. Hutson, *The Journal of Chemical Physics* **101**, 8351 (1994).
- ²⁶Y. Xu and W. Jäger, *Journal of Molecular Structure* **599**, 211 (2001).
- ²⁷A. R. W. McKellar, *The Journal of Chemical Physics* **125**, 114310 (2006).
- ²⁸G. Yan, M. Yang, and D. Xie, *The Journal of Chemical Physics* **109**, 10284 (1998).
- ²⁹F. Negri, F. Ancilotto, G. Mistura, and F. Toigo, *The Journal of Chemical Physics* **111**, 6439 (1999).
- ³⁰T. Korona, R. Moszynski, F. Thibault, J.-M. Launay, B. Bussery-Honvault, J. Boisssoles, and P. E. S. Wormer, *The Journal of Chemical Physics* **115**, 3074 (2001).
- ³¹J. Boisssoles, F. Thibault, R. Le Doucen, V. Menoux, and C. Boulet, *The Journal of Chemical Physics* **101**, 6552 (1994).
- ³²H. Li and R. J. Le Roy, *Physical Chemistry Chemical Physics* **10**, 4128 (2008).
- ³³T. Selim, A. Christianen, A. van der Avoird, and G. C. Groenenboom, *The Journal of Chemical Physics* **155**, 034105 (2021).
- ³⁴G. Guelachvili, *Journal of Molecular Spectroscopy* **79**, 72 (1980).
- ³⁵G. Chałasiński, J. Rak, M. M. Szczęśniak, and S. M. Cybulski, *The Journal of Chemical Physics* **106**, 3301 (1997).
- ³⁶K. A. Peterson, D. E. Woon, and T. H. Dunning, *The Journal of Chemical Physics* **100**, 7410 (1994).
- ³⁷S. Boys and F. Bernardi, *Molecular Physics* **19**, 553 (1970).
- ³⁸H.-J. Werner, "Molpro, a package of ab initio programs, version 2010.1, 2010,".
- ³⁹F. Lique and A. Faure, eds., *Gas-Phase Chemistry in Space*, 2514-3433 (IOP Publishing, 2019).
- ⁴⁰J. Hutson, "BOUND computer code, version 5, distributed by Collaborative Computational Project No.6 of the Science and Engineering Research Council," (1993).
- ⁴¹D. E. Manolopoulos, *The Journal of Chemical Physics* **85**, 6425 (1986).
- ⁴²L. S. Rothman and L. D. Young, *Journal of Quantitative Spectroscopy and Radiative Transfer* **25**, 505 (1981).
- ⁴³G. Graner, C. Rossetti, and D. Bailly, *Molecular Physics* **58**, 627 (1986).
- ⁴⁴T. L. Wilson, *Annual Review of Astronomy and Astrophysics* **32**, 191 (1994).
- ⁴⁵J. Hutson and S. Green, "Molscat computer program, version 14, distributed by Collaborative Computational Project No. 6 of the UK Science and Engineering Research Council," Collaborative Computational Project No. 6 of the UK Science and Engineering Research Council (1994).
- ⁴⁶A. a. Arthurs, Dalgarno, *Proceedings of the Royal Society of London. Series A. Mathematical and Physical Sciences* **256**, 540 (1960).
- ⁴⁷M. Costes and C. Naulin, *Chemical Science* **7**, 2462 (2016).
- ⁴⁸J. A. Miller, R. J. Kee, and C. K. Westbrook, *Annual Review of Physical Chemistry* **41**, 345 (1990).



$\theta = 0^\circ$  $\theta = 30^\circ$  $\theta = 60^\circ$  $\theta = 90^\circ$ 